

# Drill String Mechanics and Extension Capacity of Extended-Reach Well

Weikai LIU, Zhimin TIAN, Yueqing XU, Min ZHAO, Runqi LI, Haibo PANG, Hongyan ZHAO, Ziming FENG\*

**Abstract:** For the design and construction of the extended-reach well, the ultimate elongation capacity of the extended-reach well was studied. Given the drilling practice of extended-reach well, the extension limit prediction criterion of extended-reach well is established. In this paper, based on the drilling practice of extended-reach well, by the finite element method, the gap element method and the dynamic finite element method of the whole drill string, static analysis model of the extended-reach well and the mechanics' analysis model of drill string vibration are established. The frictional resistance condition and strength condition of the limit extension of the extended-reach well are solved respectively, and the extended limit prediction criterion of the extended-reach well is established. The software was prepared based on the model and theory, the model and software were validated with the example of drilling, and the average error of the calculated value is 6.94% when compared with the measured values in the field. It can meet the needs of drilling engineering and study of the extension capability of the extended-reach wells.

**Keywords:** drill string; extended-reach well; extension; friction; mechanics

## 1 INTRODUCTION

Over the past 20 years, the drilling technology of the extended-reach well with a ratio of horizontal length to the vertical depth greater than 2 has been greatly developed. However, issues such as wellbore cleanliness, borehole wall stability, casing penetration, and friction torque in the extended-reach well have become prominent. Especially in design and construction, the extension capacity of the extended-reach well is an urgent problem to be solved in the engineering. Regarding the extensional capacity of the extended-reach well, including modeling and solving, drill string mechanics needs to be studied in depth.

Lubinski [1] is the first major representative to propose and study drill string theory since in 1950 he published several papers on drill string theory. Lubinski A and Woods HB [2-5] have realized that the actual borehole is inclined by investigation and experiment of the practical situation on the spot. The drill string will contact the wellbore wall at the particular point of the bit (this point is referred to as the upper tangent point), and the drill string above the upper tangent point shall be pressed against the lower wellbore wall. In the 1960s, Finnie, Bailey, and Dareing [6-8] mainly performed experiments and analysis for the longitudinal vibration and the torsional vibration of the drill string in the straight well. In the 1970s, Walker BH [9] studied the force and deformation of the two-dimensional bottom hole drill assembly by using the principle of minimum potential energy. He proposed the concept of bit dip angle (the angle between the perpendicular of the bit bottom and the borehole axis). The use of energy method breaks the previous solution to the single differential equation, which opens up an approximate calculation precedent for drill string mechanics. In 1977, Bai Jiazhi [10] proposed the theory of crossbar bent continuous beam to solve the force and deformation of the bottom hole drill assembly. He generalized this method from one-dimensional situation to three-dimensional situation in the future study. In 1978, Millheim K. K. [11-13] et al. initially established the finite element three-dimensional static model for the bottom hole drill assembly analysis. They used the space beam unit as the basic unit and used the gap element (GAP) to simulate the contact condition between the drill string and the

borehole wall. In the 1980s, Millheim and Apostol [14-16] systematically studied the vibration of the drill string for the first time. Based on the original static analysis, inertial forces and friction forces were introduced to establish the three-dimensional finite element model for dynamic analysis of downhole drilling tools. In 1984, Dunayevsky [17, 18] et al. studied the conditions of vibration in a directional well using a tri-cone drill bit and the stability of the drill string, and determined the relationship between parametric resonance area of the drill string vibration and the rotating speed, firstly pointing out that the drill string not only rotates around its axis, but also there is vibration at the same time. In the early 1990s, Shuai [19] et al. regarded the effect of the deformation of the drill string in response to the shape of the wellbore as the initial stress and took it into account, considered the effect of bending joint as the initial displacement in the three-dimensional static analysis of bottom hole drill assembly in directional wells using the finite element method.

In this century, G. Ooms and B. E. Kampman-Reinhartz [20] analyzed the effect of the drill string on the pressure drop of Newtonian liquid during the eccentric rotation of the drilling process. G. Heisig [21] et al. studied the lateral vibration of the drill string which is in contact with the borehole wall in the horizontal well and analyzed its inherent frequency by the analytical method. In 2001, Liu [22] et al. simplified the drill bit and drill string as a spring-resistance-mass system and established a dynamic model of transverse vibration of roller bit based on the interaction between the drill string and the rock. In 2003, Guan [23] et al. designed and established a bottom drill string dynamics research and test device with a geometry size of 1:10. Using this device, the experiments of motion features of the bottom drill string of a vertical well were performed under the condition of diverse WOB and rotat speed. In 2005, Han [24, 25] et al. analyzed the torsion, longitudinal and lateral vibrations of the drill string through the microelement linear analysis method, and explored the law of vibration. G. Rae [26] et al. analyzed and studied the successful drilling of the extended-reach well of the CAPTION oil field in Beihai, summarized the definition of torque and resistance analysis and its importance, and summarized the application of torque and resistance analysis in drilling operations. In 2006, S. S. Janwadkar

and D. G. Fortenberry [27] studied drilling problems in the Nade shale oilfield in North Texas. They use detailed BHA and drill string model software for detailed engineering analysis. The created model helps design the BHA. The new BHA reduces drill string bending and greatly reduces the torque and drag of bending and lateral parts of the drill string. Bakke [28] used data statistics to study the current laws of drilling extension limits. The maximum extension limit for horizontal displacement is mainly concentrated at a vertical depth of 5000-1000 ft. Abahusagy [29] analyzed the effects of various measures to increase the extension limit in the successful completion of the Nikaitchuq extended-reach well. In 2013 Vestavik [30] proposed the use of double-wall drill pipe drilling technology to increase the borehole extension limit. In 2014, Gradishar [31] pointed out the influence of various factors on the extension limit of drilling through the drilling history of an offshore extended-reach well. In 2018, Xin Li [32] proposed an optimal design principle and control method for the subjective and objective constraints of the bare-hole extension limit for large displacement horizontal wells with the goal of improving the bare-hole extension limit. In 2020, Huang W. J. et al. [33], constructed a tubular column segmentation optimization design method based on the extension limit of large displacement wells by considering the influence of various operating conditions and constraints of the tubular column. The new design method can effectively solve the problem of optimized design of tubular columns and joints in large displacement wells.

The above-mentioned investigations have in-depth study of the mechanical problems and extensional capacity of drill string in the extended-reach well, involving the statics and dynamics of the drill string, theoretical analysis, and engineering practice. However, there is no systematic study on the drill string mechanics for the extension ability limit of the extended-reach wells. The static and dynamics of the drill string of the extended-reach wells are not combined to consider the extension problems. Therefore, with the continuous increment in the number of the extended-reach wells, there is an urgent need for a complete theoretical solution to the problem of extension ability of the extended-reach wells. In this paper, from the drilling practice of the extended-reach wells, based on the finite element method, the gap element method and the dynamic finite element method of the overall drill string, the static and dynamic analysis models of the extended-reach well is given, the prediction criterion of the extension limit of the extended-reach well is established and the real-drilled extended-reach wells have been calculated and analyzed.

## 2 EXTENSION LIMIT PREDICTION CRITERIA FOR THE EXTENDED-REACH WELLS

In the extended-reach wells, they may affect the horizontal extension of the drill string due to wellbore profile, wellbore geometry features, wellbore cleaning, drill string structure, drilling fluid properties, and rock drillability. In particular, due to the long drill string of the extended-reach wells, the resistance to the drill string is relatively large, and the horizontal length has affected the continued drilling. The main consideration here is rock crushing, frictional resistance, drill string strength, and

drill string stiffness. To ensure the smooth penetration of drill string, the following requirements usually need to be met.

### 2.1 Rock Crushing Conditions

The WOB and torque at the drill bit need to be greater than the maximum strength of the rock against damage. When the drill bit breaks the rock, the load on the drill bit needs to be greater than the threshold load, that is to say, the pressure of bit exerted by drill string needs to be greater than this threshold value. Otherwise, the drill bit cannot penetrate. In summary, the following formulas can be given:

$$F_{\text{bit}} \geq F_{\text{threshold}}(T, R, E) \quad (1)$$

In the formula:  $F_{\text{bit}}$  - indicates bit load, kN;  $F_{\text{threshold}}(T, R, E)$  - indicates the rock threshold pressure, which is a function of  $T$  (the shape of the teeth of the drill),  $R$  (the nature of the rock), and  $E$  (the environmental condition), kN.

### 2.2 Drill String Friction Resistance Conditions

Factors affecting the extension of the extended-reach wells, besides the ability of the drill bit to break rocks, the main factor is the friction resistance of drill string in the extended-reach wells. The effect of frictional resistance on the extension of the extended-reach wells is mainly due to the fact that frictional resistance consumes the effective weight of the drill string, so that the drill bit cannot get enough WOB, the drill bit cannot crush the rock, and the drill string cannot continue drilling, indicating this drill bit assembly has reached the limit of extension. It can be said that the frictional resistance of the drill string has the greatest influence on the extension ability of the extended-reach wells. If the extension distance of the extended-reach wells is to be increased, the most fundamental solution is to reduce the frictional resistance of the drill string. Comprehensively lifting, down-pass, orientation, rotary table drilling, and other conditions, the formula for drilling string to overcome the friction resistance and continue drilling can be obtained:

$$F_{X'}^{\text{en}} + F_{X'}^{\text{e}(n+1)} + T_{X'_{\text{max}}}^{\text{en}} < 0 \text{ lifting condition} \quad (2)$$

$$F_{X'}^{\text{en}} + F_{X'}^{\text{e}(n+1)} + T_{X'_{\text{max}}}^{\text{en}} < 0 \text{ other condition} \quad (3)$$

Among them:  $F_{X'}^{\text{en}}, F_{X'}^{\text{e}(n+1)}, T_{X'_{\text{max}}}^{\text{en}}$  indicate the external force received by the drill string unit in the axial direction near the wellhead end, the external force received in the axial direction of the drill bit end and the frictional resistance in the axial direction are positive in the bottom hole direction.

In addition to the consideration of the force in the axial direction during the rotary table penetration, the torque problem must also be considered. During rotary table drilling, the entire drilling tool rotates, and the drill string withstands the largest torque at the wellhead and the

minimum at the bit, in other words, the maximum torque  $M_{max}$  that the rotary table can provide is greater than the torque  $M_X$  at the wellhead, and the drill is considered to satisfy the torque condition.

$$M_{max} > M_X \tag{4}$$

### 2.3 Drill String Strength Conditions

The working stress in each section of the drilling tool must be less than the allowable stress of the material to ensure that the drill tools will not break or fail. In drilling operations, the drill string is used to transmit the WOB and torque, so the drill string cannot cause problems and must be secured. Therefore, any part of the drill string must be inspected to meet the strength requirements. The formula is as follows:

$$\sigma_i \leq [\sigma] \tag{5}$$

In the formula:  $\sigma_i$  - is the stress of the  $i$ -th section of the drill string.  $[\sigma]$  - is the allowable stress of drill string material.

### 2.4 Drill String Stiffness Conditions

The bending deformation of the drilling tool should be less than the allowable deformation value of the drilling tool to ensure that the drilling tool can work normally. Each drilling tool has a certain degree of allowable deformation and cannot exceed this range. Once this range is exceeded, the drilling tool will not work properly. There are formulas for this:

$$\theta_i \leq [\theta] \tag{6}$$

In the formula:  $\theta_i$  - is the deformation value of the  $i$ -th section of the drill string.  $[\theta]$  - is the allowable value of drill string deformation.

Generally, drilling tools can satisfy this requirement and are not usually used as a criterion for determining extensional limit models for the extended-reach wells.

Based on these four aspects, the formula for determining the extension limit is obtained as follows:

$$\begin{cases} F_{bit} \geq F_{threshold}(T, R, E); \\ F_{X'}^{en} + F_{X'}^{e(n+1)} + \Delta F_{X'}^{en} + F_{X'_{max}}^{en} < 0 \text{ lifting condition} \\ F_{X'}^{en} + F_{X'}^{e(n+1)} + \Delta F_{X'}^{en} + F_{X'_{max}}^{en} > 0 \text{ other conditions} \\ M_{max} > M_X \text{ rotary table penetration} \\ \sigma \leq [\sigma] \end{cases} \tag{7}$$

In addition to this, the capacity of the drilling rig and the running capacity of the casing need to be considered. If the drill string satisfies these requirements, it is assumed that the drill string can continue to penetrate, and as long as it is not satisfied on one hand, it is considered to have reached the extension limit value of drill string.

Based on this understanding, it can be seen that it is necessary to study the stress state and the friction condition of the drill string section. Only by determining the force state of the cross-section can the extension limit of the drill string be given. Therefore, the above mechanical analysis is the basis for solving the drill string stretching ability of the extended-reach wells.

## 3 DRILL STRING MECHANICS ANALYSIS OF THE EXTENDED-REACH WELLS

### 3.1 Static Analysis of Drill String in Extended Displacement Well

#### 3.1.1 Establish a Simplified Model

By analyzing the working conditions of the drill string in the extended-reach wells, a schematic diagram of the mechanics' analysis model of the drill string for the extended-reach wells is shown in Fig.1. In constructing the model of Fig.1, based on the whole drill string in three-dimensional space from the wellhead to the downhole drill bit, the following assumptions are used: (1) The drill string of the extended-reach well is an elastic deformable body; (2) The inner borehole wall is rigid, and the wellbore is circular; (3) The contact between the drill string and the wellbore wall is random, the contact deformation belongs to the elastic deformation range, and the contact has the effect of contact reaction force and frictional resistance; (4) Ignore the influence of all dynamics factors.

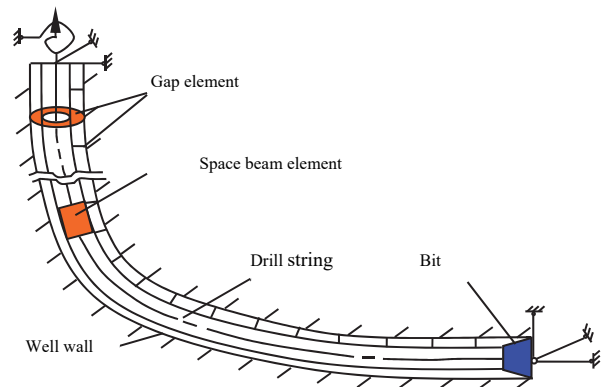


Figure 1 Simplified model for frictional resistance mechanical analysis of drill string in extended-reach well

The model in Fig. 1 also considers the spatial structure of wellbore in the extended-reach well, whose axis is an arbitrary three-dimensional curve in space. The borehole axis spatial position is determined by the wellbore design or measured well depth, well angle and azimuth data obtained from actual drilling which are calculated by spline function interpolation. The wellbore diameter of the extended-reach well can be arbitrarily changed through the wellbore, and the structure and size of the drill string of the extended-reach well can be changed arbitrarily.

The boundary conditions are treated with as follows: when the rotary table drilling tool is used for drilling, the displacement and rotation angle are free along the axis at the wellhead and fixed in other directions; in addition to the free lateral rotation angle the displacement of drill bit at the bottom of the well is fixed in other directions. When the power drilling tool is drilled, the wellhead is simplified into a fixed end; the three linear displacements of the well bottom drill bit are fixed, the axial torque is known, and the



In the formula,  $EA$  is the tension-compression stiffness,  $EI$  is the bending stiffness,  $GI_p$  is the torsion stiffness,  $b_1 = 1 + \frac{12kEI}{GAL^2}$ ,  $b_2 = 4 + \frac{12kEI}{GAL^2}$ ,  $b_3 = 2 - \frac{12kEI}{GAL^2}$ ,  $k$  is the shear stress distribution non-uniform coefficient of the section. When  $L$  is long enough,  $\frac{12kEI}{GAL^2}$  is very small.

From the transformation of element node displacement and nodal force vector in the local coordinate system to the element node displacement and nodal force vector in the total coordinate system, the conversion relationship between unit stiffness matrix  $A$  in the total coordinate system and the element stiffness matrix in the local coordinate system is:

$$[K_0]^e = [T]^{-1} [K_0']^e [T] \tag{15}$$

Then the matrix equations of all units are converted to coordinate systems in the total coordinate system according to Eqs. (9) and (15), and then a series of calculations and assembly are performed by the superposition principle, and the overall balance equation of drill string of an extended-reach well will be obtained:

$$[K_0] \{\delta\} = \{F\} \tag{16}$$

In the formula,  $[K_0]$ ,  $\{\delta\}$  and  $\{F\}$  is the overall stiffness matrix, nodal displacement, and nodal force vector for the drill string total coordinate system in the extended-reach well respectively.

### 3.1.2.2 Gap Element Model

Eq. (16) does not consider the contact and friction between the drill string and the borehole wall, which will cause singularity when used. Applying the gap element theory not only can accurately and conveniently describe the random contact friction state between the drill string and the borehole wall, but also can solve the singular problem of the total stiffness matrix of the drill string in the extended-reach wells.

The multi-directional contact friction gap unit is a virtual unit composed of liquid or gas. The outer boundary is connected with the well wall, and the inner boundary is connected with the drill string. The geometric shape is a thick circle. The unit has the following physical characteristics: When the drill string is not in contact with the borehole wall, it does not affect the free movement of the drill string, and its compression stiffness is close to zero; if it is in contact, the gap unit compresses along a certain radial direction on the wellbore circumference, the inside and outside boundary of gap elements are tangent at the contact point. Its compressive stiffness is equal to a given value or becomes large enough to prevent mutual penetration of the drill string and the borehole wall, but allows the drill string to slide along the well wall under the action of contact reaction force, frictional resistance and resistance moment.

For the static finite element analysis is of the extended-reach wells, the gap elements are set up at the nodes of the drill string elements, and each node is provided with a gap

element. Each point where the drill string comes in contact with the borehole wall is a local geometrically non-linear problem and the locations of the contact points are random, as shown in Fig. 2.

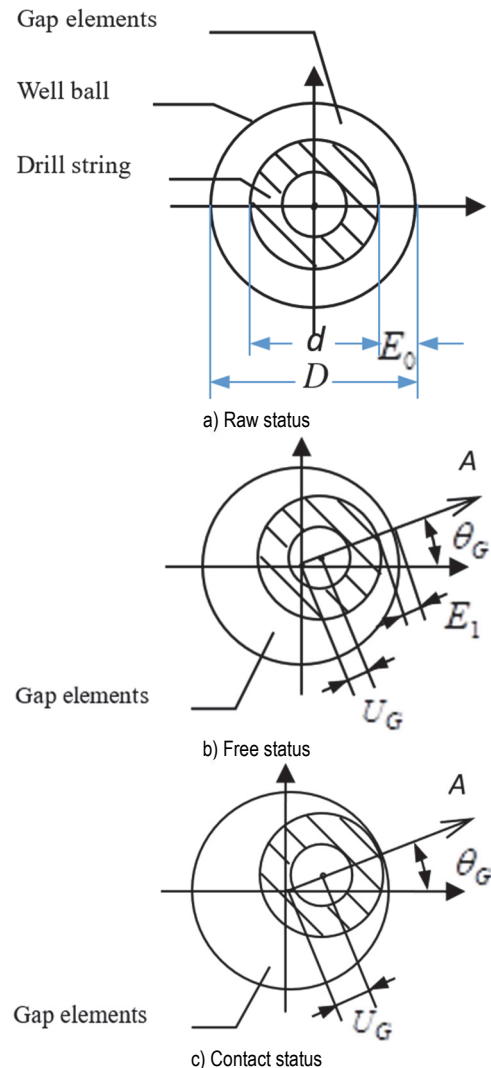


Figure 2 Gap elements model

In Fig. 2, if the drill string produces a maximum compressive deformation  $U_G$  in a direction  $A$  of the gap element circumference, that is, the displacement of the gap element in the direction  $A$  is  $U_G$ , the deformation in this direction represents the deformation of the gap element, the direction angle  $\theta_G$  of  $A$  indicates the direction of the contact point of the gap element. Let the initial gap of the gap element be  $E_0$ , and the gap after deformation be  $E_1$ , then:

$$E_1 = E_0 - U_G \tag{17}$$

Judging criteria for displacement of the drill string in contact with the well wall: When  $0 < E_1 \leq E_0$ , there is no contact between the drill string and the wellbore of the extended-reach well; when  $E_1 = 0$ , the drill string of the extended-reach well contacts the well wall. Internal force conditions of contact: When no contact occurs,  $R_{normal} = 0$ ,  $R_{axis} = 0$ ,  $R_{tangent} = 0$ ,  $m = 0$ ; when contact occurs,  $R_{normal} = K_{gap}U_G$ ,  $R_{axis} = f_{axis}R_{normal}$ ,  $R_{tangent} = f_{tangent}R_{normal}$ ,  $m = 0.5R_{tangent}d$ . In the formula,  $R_{normal}$ ,  $R_{axis}$ ,  $R_{tangent}$ ,  $m$  is the

normal contact reaction force, circumferential contact frictional resistance, tangential contact frictional resistance, and rotational resistance moment of the  $i$ -th gap element respectively;  $f_{axis}$ ,  $f_{tangent}$ ,  $d$  is the axial friction factor, tangential friction factor, and outer diameter of the gap element respectively, among them  $f = \sqrt{f_{axis}^2 + f_{tangent}^2}$ ,  $f_{axis}/f_{tangent} = v_{axis}/v_{tangent}$ , and  $f$  is the friction factor of the gap element in the extended-reach wells,  $v_{axis}$ ,  $v_{tangent}$  is the axial speed and tangential speed of the outer diameter of the unit drill string. It can be seen that the stiffness of the gap element is variable, and its change should meet the contact conditions of the unit in which it is located and the corresponding contact force conditions.

The principle of minimum potential energy was used to derive the unit equilibrium equation in the local coordinate system. After the calculations such as coordinate conversion and superposition principle, the overall balance equation of the drill string contact system of the extended-reach well can be obtained:

$$[K]\{\delta\} = \{F\} \tag{18}$$

In the formula,  $[K]$  is the overall stiffness matrix of the drill string of the extended-reach wells with gap elements.  $\{F\}$  is the nodal force vector in the global coordinate system where frictional resistance and drag torques have been considered. Due to the introduction of gap elements, the overall stiffness matrix  $[K]$  in Eq. (10) is a non-singular matrix and can be solved by applying iterative methods.

### 3.2 Drill String Vibration Analysis of Extended-Reach Wells

#### 3.2.1 Mechanical Analysis Model of Drill String Vibration in the Extended-Reach Wells

The vibration problem of the drill string in the extended-reach wells is closely related to the length and shape of the overall drill string. Vibration analysis must use the overall drill string as the mechanical model, the whole drill string from the wellhead to the bottom of the well as the research object, as shown in Fig. 3.

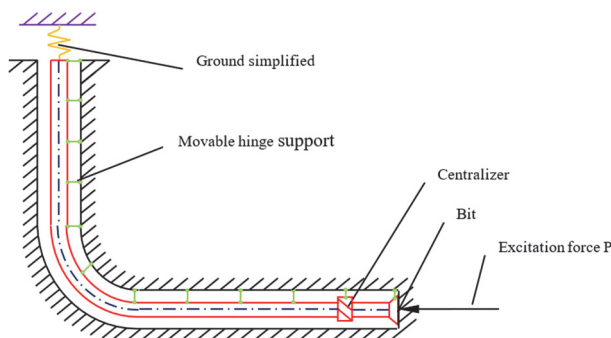


Figure 3 Schematic diagram of the drilling string structural unit for extended-reach wells

It can be composed of any combination of different drill accessories, such as drill collars, drill pipes, joints, centralizers, and shock absorbers. Meanwhile, the influence of the ground structure on the vibration of the drill string should be considered. The derrick, steel wire rope, and traveling tackle and other ground structures are simplified into an equivalent axially free-movable but no

lateral movable structure. The contact between the drill string and the well wall is considered as a movable hinge support. The drill string of the extended-reach well is considered to be a three-dimensional space column that coincides with the wellbore axis, and the effect of bending stress caused by the initial curvature of the drill string on the fatigue strength of the drill string should also be considered.

In forced vibration of a structural system, the structural system starts to vibrate from the application of excitation force. In a short period of time after starting vibration, the vibration system includes two parts: one is the free vibration part; the other is the forced vibration part. Due to the effect of the damping force, as time increases, the free vibration part of the structural system will gradually attenuate and disappear after a certain time, leaving only the steady-state forced vibration of the structural system. From the moment the excitation force acts on the steady-state forced vibration, it can be called the system's transient forced vibration, which is a very complicated vibration state. The vibration of the drill string system discussed here is limited to the steady-state forced vibration. The previous studies have shown that it can be approximately assumed that the inherent frequencies and inherent vibration modes of structural systems are not affected by damping, but are only related to the system structure itself.

#### 3.2.2 Finite Element Equation of Drill String Vibration in the Extended-Reach Wells

Based on the above drill string mechanics models of the extended-reach well, the drill string of the extended-reach well is dispersed into multiple spatial beam units along the axis. Vibration analysis is performed using the dynamic finite element method to obtain the vibration equation of the overall drill string structure:

$$MU'' + CU' + KU = P_0 \sin(\omega t) \tag{19}$$

In the formula,  $M$ ,  $C$ ,  $K$  are the overall mass matrix, the damping matrix and the stiffness matrix of the overall drill string, respectively.  $P_0$  is the excitation force amplitude.  $\omega$  is the excitation frequency.  $t$  is the time variable.  $U''$ ,  $U'$ ,  $U$  are the node acceleration vector, the velocity vector, and the displacement vector, respectively.

It is important to note that the factors influencing the magnitude and frequency of the drill string excitation force are very complex. The amplitude and frequency of the excitation force are not only related to the bit structure and the drilling tool structure, but are also related to the nature of the formation and drilling parameters. It is assumed that the excitation force is simple harmonic excitation force. For a tri-cone bit, in the relatively stable drilling process, it is generally assumed that the frequency of the excitation force acting on the drill bit is three times the drill string rotation frequency, which is an accepted practical assumption in the general drill string vibration analysis. For the PDC bit, it differs from that of the tri-cone bit, so its excitation force frequency is different from the frequency of the excitation force of the tri-cone bit and needs to be determined by simulation experiments.

Although the frictional contact resistance between the drill string and the borehole wall is not large, it is different

from general mud damping. Rayleigh damping is used for calculation convenience. Assume that the damping matrix is:

$$C = C_1 + C_2 \tag{20}$$

In the formula,  $C_1$  is mud damping and structural damping,  $C_1 = \alpha M + \beta K$ , in the formula, the right-side term coefficients  $\alpha$  and  $\beta$  are arbitrary proportional coefficients.  $C_2$  is the damping caused by frictional contact resistance.

$$C_2 U' = R_t \tag{21}$$

In the formula,  $R_t$  indicates the contact frictional resistance vector, where each element represents the frictional resistance at the corresponding node and is derived from the drill above string static analysis of the extended-reach well and then converted to an equivalent diagonal damping matrix based on the nodal speed.

To solve the Eq. (19) by using the vibration mode superposition method, the intrinsic frequency and intrinsic vibration mode of the drill string must first be determined. Hence, the undamped free vibration equation must first be solved as follows:

$$MU'' + KU = 0 \tag{22}$$

Set the form of the solution is

$$U = \Phi \sin(\omega t) \tag{23}$$

From this formula, the frequency equation can be obtained as:

$$K - \omega^2 M = 0 \tag{24}$$

And then, the  $n$  inherent frequencies of the drill string structure can be obtained, and the  $n$  inherent frequencies can be ranked from small to large:

$$\omega_1 < \omega_2 < \omega_3 \dots < \omega_n \tag{25}$$

It is further possible to find  $n$  inherent modes  $\Phi_i$  ( $i = 1, 2, \dots, n$ ) corresponding to the  $n$  inherent frequencies.

Afterward, using the mode superposition method, the  $n$  independent second-order linear non-homogeneous differential equations of Eq. (19) can be obtained:

$$y_j'' + 2\omega_j \gamma_j y_j' + \omega_j^2 y_j = P_j^* \sin \omega_0 t \tag{26}$$

$(j = 1, 2, \dots, m)$

In the formula,  $\gamma_i = \frac{\beta + \alpha \omega_i^2}{2\omega_i}$  ( $i = 1, 2, \dots, m$ ) is the

$i$ -th mode damping ratio.

Its special solution is:

$$y_j = A_j \sin \omega_0 t + B_j \cos \omega_0 t \tag{27}$$

In the formula:

$$\left. \begin{aligned} A_j &= \frac{P_j^*}{\omega_j^2} \frac{1 - \frac{\omega_0^2}{\omega_j^2}}{\left(1 - \frac{\omega_0^2}{\omega_j^2}\right)^2 + \left(2\gamma_j \frac{\omega_0}{\omega_j}\right)^2} \\ B_j &= \frac{-P_j^*}{\omega_j^2} \frac{2\gamma_j \frac{\omega_0}{\omega_j}}{\left(1 - \frac{\omega_0^2}{\omega_j^2}\right)^2 + \left(2\gamma_j \frac{\omega_0}{\omega_j}\right)^2} \end{aligned} \right\} (j = 1, 2, \dots, m) \tag{28}$$

In this way, the displacement response of the drill string is:

$$U = \phi A \sin(\omega_0 t) + B \cos(\omega_0 t) \tag{29}$$

Based on this, the response internal force and response stress can be further calculated as a basis for assessing the dynamic strength of the drill string.

### 3.2.3 Fatigue Strength Analysis and Calculation of Drill String in the Extended-Reach Wells

Since the forces on the drill string, there are relatively complex, tensile, pressure, bending and torsional stresses. In this paper we believe that the axial tension and pressure work stress is the main stress of fatigue damage, while the lateral bending dynamic stress is limited by the wellbore, the value is smaller, it is the secondary stress of fatigue failure (it can also be equivalently reduced and then added to the tension and pressure dynamic stress). The torsional stress is much smaller than tensile and compressive stress, and can be neglected. Therefore, drill string fatigue is mainly caused by normal longitudinal stress.

#### 3.2.3.1 Calculation of Cross-Sectional Stress of Drill String

##### 3.2.3.1.1 Drill String Pre-Tightening Stress

Under the action of the buckle pre-tightening torque, the tensile pre-tightening stress generated near the deduction stress groove of the pin and the root of the screw thread is as following:

$$\sigma_y = \frac{M_0}{2fRA_0} \tag{30}$$

In the formula:  $M_0$  - is the screw on pre-tightening torque, which is related to the drill collar, the drill pipe type, and the thread type,  $f$  - is the drill string surface contact friction coefficient,  $R$  - is the root diameter of the thread,  $A_0$  - is the cross-sectional area of the root of the thread.

##### 3.2.3.1.2 Working Static Stress of Drill String

Under the action of the average WOB and self-weight, the cross-section of the drill string will produce normal tensile stress, and its calculation formula is:

$$\sigma_p = \frac{N_J}{A} \quad (31)$$

In the formula:  $N_J$  - is static axial force;  $A$  - is the cross-sectional area of the drill string. If it is a joint, it is the effective cross-sectional area of the screw.

### 3.2.3.1.3 Normal Stress Amplitude of Drill String Vibration

From the analysis of the drill string vibration, the harmonic alternating axial amplitude  $N_D$  of the longitudinal vibration of the drill string can be obtained. Based on this, the positive stress amplitude of the drill string vibration can be calculated as:

$$\sigma_1 = \frac{N_D}{A} \quad (32)$$

This stress is a major factor in the fatigue failure of the drill string.

### 3.2.3.1.4 Initial Bending Normal Stress of Drill String

In an extended-reach well, the initial bending stress at the deflected section is large, so this part of the stress is important, and its magnitude is related to the borehole curvature. The initial bending normal stress of the drill string caused by the borehole curvature is:

$$\sigma_0 = \frac{DE}{2\rho} \quad (33)$$

In the formula:  $\rho$  - is the radius of borehole curvature;  $D$  - is the outer diameter of the drill string;  $E$  - is the elastic modulus of the drill string material. The initial bending normal stress of the drill string is an alternating normal stress when the rotary table is drilled, which belongs to dynamic stress; it is a constant normal stress when directional drilling, and belongs to static stress.

### 3.2.3.1.5 Calculation of Cross-Sectional Stress of Drill String

The cross-sectional stress of the drill string can be divided into two parts: one is the average stress  $\sigma_m$ , and the other is the alternating stress amplitude  $\sigma_a$ . If the power drill is used, the impact of power drill rotation should also be considered.

When the rotary table does not rotate:

$$\sigma_m = \sigma_y + \sigma_p + \sigma_0, \quad \sigma_a = \sigma_1 \quad (34)$$

When the rotary table rotates:

$$\sigma_m = \sigma_y + \sigma_p, \quad \sigma_a = \sigma_1 + \lambda\sigma_0 \quad (35)$$

where  $\lambda$  is the ratio of the rotary frequency of the rotary table to the frequency of the drill's excitation force.

### 3.2.3.2 Drill String Fatigue Strength Conditions

During the operation of the drill string, each cross-sectional stress is in a typical asymmetric cycle. Under certain cyclic characteristics  $r$ , the permissible fatigue (permanent) limit of a section of the drill string is calculated by the following formula:

$$[\sigma_r] = \frac{2[\sigma_{+1}][\sigma_{-1}]}{(1-r)[\sigma_{+1}] + (1+r)[\sigma_{-1}]} \quad (36)$$

$$r = \frac{\sigma_m - \sigma_a}{\sigma_m + \sigma_a} \quad (37)$$

In the formula:  $r$  - is the asymmetry stress cycle eigenvalue;  $[\sigma_{+1}]$  - is the allowable stress for a constant (static) load;  $[\sigma_{-1}]$  - is the permissible endurance limit of the drill string under symmetric stress cycling state.

Because the drill string alternating load is not stable, it may change along with the impact, so the allowable endurance limit should also be divided by the additional safety coefficient  $n_f$ , the value of this coefficient is changed with the asymmetry, the stress changes more dramatic, the higher the coefficient, it is taken as 1.2 here. In this way, the permissible endurance limit of the drill string structure can be obtained, and the following drill string fatigue strength conditions are established according to this:

$$\sigma_{\max} = \sigma_m + \sigma_a \leq [\sigma_r] \quad (38)$$

Here  $\sigma_{\max}$  is the maximum working stress of the drill string. If the drill string has a cross-section that does not meet the fatigue strength condition Eq. (38), it is considered that the drill string will produce fatigue fracture, and Eq.a (38) is the basis for the fatigue safety assessment of the drill string.

For the drill string of an extended-reach well, the sections at different depths of the well have different working stress, and its stress cycle characteristic value  $r$  is also different. The permissible endurance limit  $[\sigma_r]$  is also different because  $r$  and  $[\sigma_r]$  are related to the magnitude of stress in the section. Therefore, the work stress and the permissible endurance limit of each section of the whole drill string in the extended-reach well are not the same and must be calculated one by one. Then check each part for strength conditions and combine them to arrive at a fatigue safety assessment conclusion for the entire drill string of the extension well.

## 4 CALCULATION EXAMPLES

### 4.1 Comparison of Theoretical Calculations and Actual Results of the Extended-Reach Wells

The drilling depth of the Fuping 24 well in the Jilin Oilfield was designed to be 1141.73 m, the depth of the deflecting point was 172.41 m, the vertical depth of the drilling was 388.83 m, the horizontal displacement was 848.05 m, and the maximum well angle was 92.78°. Although the well depth is not long, its ratio of well depth to vertical depth is 2.94, which is an extended-reach well.

The drill assembly in the horizontal section is:  $\Phi 215$  mm PDC bit +  $\Phi 165$  mm single-bend screw drilling tool + LWD +  $\Phi 127$  non-magnetic drill boring  $\times 1$  +  $\Phi 127$  mm heavy-duty drill pipe  $\times 2$  +  $\Phi 127$  mm slope drill pipe +  $\Phi 127$  mm heavy drill pipe  $\times 18$  +  $\Phi 165$  mm drill collar  $\times 6$  +  $\Phi 127$  mm drill pipe + 133 mm kelly stem. The drilling parameters at 1108 m depth: drilling pressure 30.00 kN; rotation speed 30 rpm; mud density 1.440 g/cm<sup>3</sup>; displacement 32 l/s.

Using the computer software compiled of the theoretical model of this paper, frictional resistance calculations were performed for the wells in the trip (lifting and lowering), the rotary table drilling, and the directional drilling during the drilling process. The software calculation process is shown in Fig. 4.

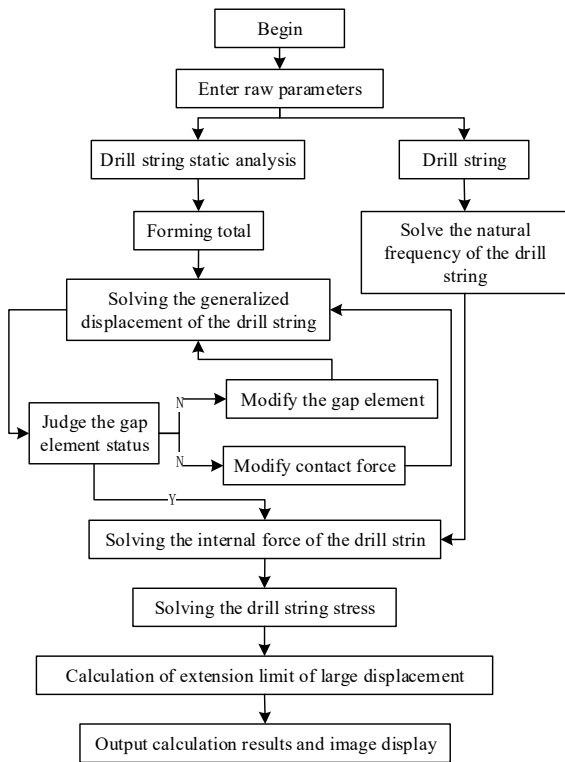


Figure 4 Software calculation flow chart

The prediction and measured results of lifting, lowering, rotary drilling, and directional drilling are shown in Tab. 1 (the values in the table with \* are total resistance torque, unit is kN.m.) The distribution curves of friction resistance along well depth during lowering, rotary drilling, and directional drilling is shown in Figs. 5 to 8.

The axial forces and axial stresses for running up and running down were also calculated separately, and the calculated results are shown in Figs. 9 to 12, respectively.

As can be seen from Tab. 1 and Fig. 5 to Fig. 8, the lifting tool is more frictional than the lower drilling tool, and the total frictional resistance in the horizontal section is much larger than the total frictional resistance in the deflected and vertical well sections. The frictional resistance within the segment is minimal. It is also known by the calculation that the axial frictional resistance of the rotary table bore is much smaller than the axial frictional resistance of the directional borehole, but the resistance torque is large.

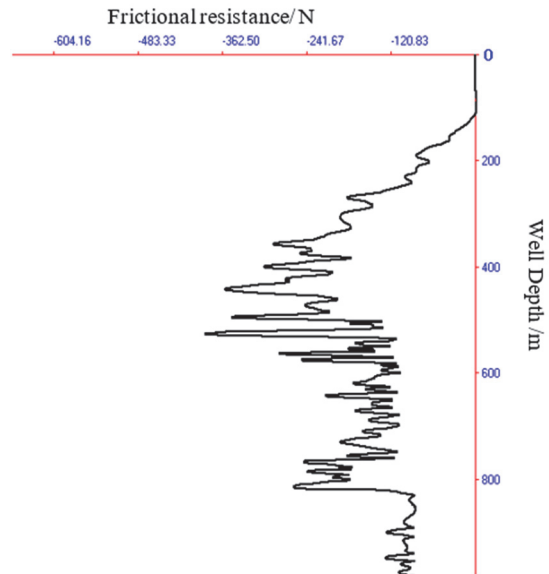


Figure 5 The distribution law of friction resistance along well depth

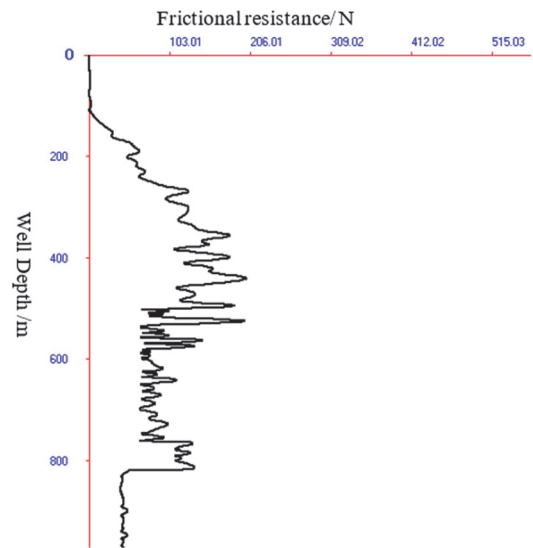


Figure 6 Distribution law of frictional resistance along well depth in lowering working conditions

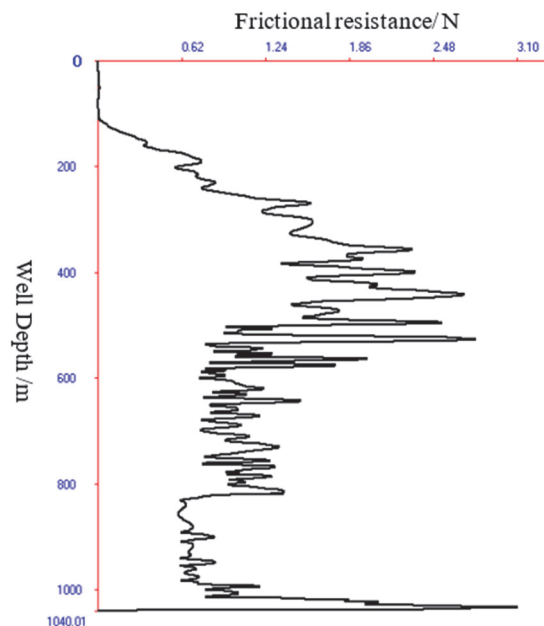
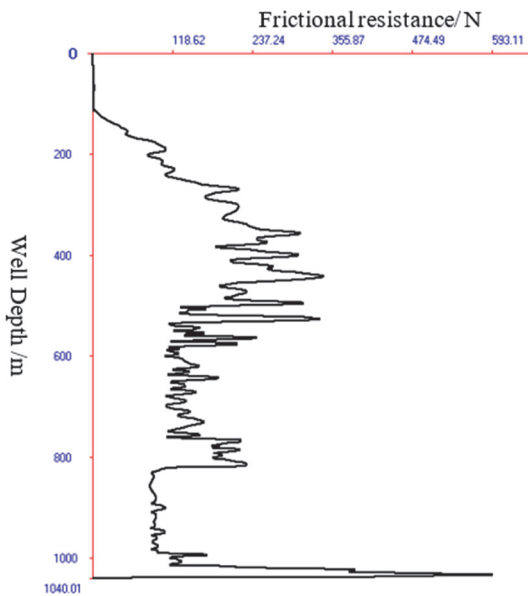


Figure 7 Distribution law of frictional resistance along the well depth in rotary table drilling

**Table 1** Comparison between friction resistance theoretical analysis and actual result of Fuping 24 well

Well depth / m	Project	Lifting	Lowering	Rotary table penetration	Directional penetration
933 ~ 943 (well angle 89.4°)	WOB / kN	0	0	30	40
	Hang weight calculation/kN	204.41	116.67	135.83	65.58
	Measured value of hang weight/kN	220	120	140	70
	Total resistance/kN	-59.18	55.32	8.86 *	64.75
	Error/%	7.09	3.11	2.98	6.32
	The fatigue safety assessment conclusions	> 1	> 1	> 1	> 1
1040 ~ 1049 (well angle 90.14°)	WOB/kN	0	0	30	40
	Hang weight calculation/kN	210.91	109.30	137.42	58.02
	Measured value of hang weight/kN	230	115	150	62
	Total resistance/kN	-67.52	63.64	9.45 *	73.93
	Error/%	8.30	4.96	8.39	6.42
	The fatigue safety assessment conclusions	> 1	> 1	> 1	> 1
1141 (well angle 85°)	WOB/kN	0	0	30	40
	Hang weight calculation/kN	213.49	96.28	134.27	44.59
	Measured value of hang weight/kN	235	105	145	50
	Total resistance/kN	-74.60	72.75	9.99 *	84.80
	Error/%	9.16	8.31	7.40	10.82
	The fatigue safety assessment conclusions	> 1	> 1	> 1	> 1



**Figure 8** Distribution law of directional drilling friction resistance along well depth

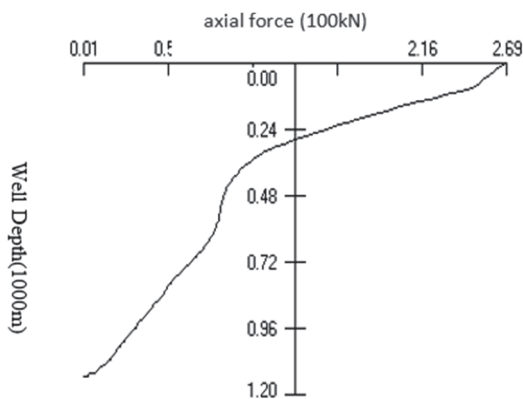


**Figure 9** Drilling tool axial force distribution along the well depth with running up drilling tools

Therefore, high-strength drill rods are used when drilling horizontal extended-reach wells. It can also be seen from Tab. 1 that the maximum error between the calculation result and the actual measurement is 10.82%, the minimum error is 2.98%, and the average error is 6.94%. It shows the correctness of the theoretical software and computer software of this paper. As seen in Figs. 9 to

12, the shaft force is not significant and the drilling column is safe.

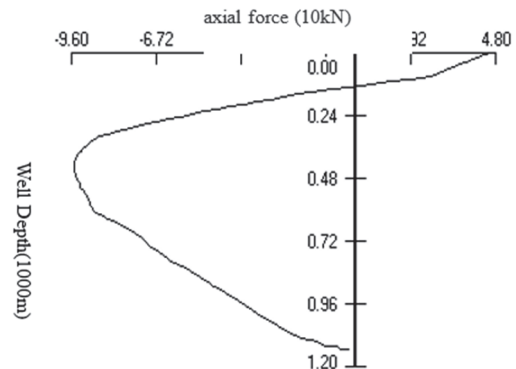


**Figure 10** Drilling tool axial force distribution along the well depth with running down drilling tools

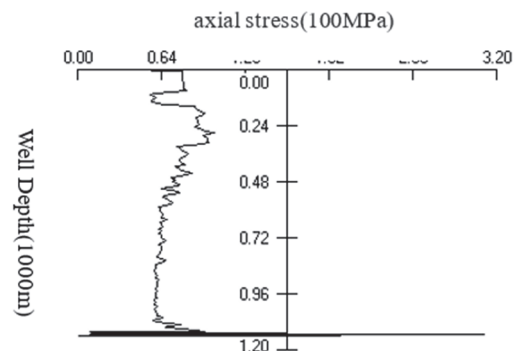


**Figure 11** Drilling tool axial stress distribution along the well depth with running up drilling tools

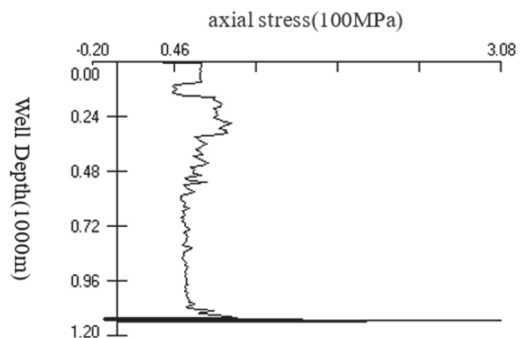


**Figure 12** Drilling tool axial stress distribution along the well depth with running down drilling tools

## 4.2 Influence Factors of Ultimate Extension Ability of the Extended-Reach Wells

The theory can also analyze and calculate the factors influencing the ultimate extension capacity. Using the Fuping 24 well to analyze several major factors affecting the extension of the extended-reach well, the following are some analysis results.

### 4.2.1 Influence of Rotating Speed on Ultimate Extension Ability of the Extended-Reach Wells

The rotary drilling and the directional drilling have different effects on the extension of the extended-reach wells. This is discussed in many works of literatures. It is often required to open the rotary table in the extended-

reach well drilling. It has greatly enhanced the extension capability for extended-reach wells. The effect of rotational speed on the extension capacity of extended-reach wells is mainly shown in that the higher the rotating speed, the smaller the axial resistance of drill string in extended-reach wells will be, but this effect on the extension capability of the extended-reach well is limited due to the higher speed running speed. The influence of rotational speed on the ultimate extension capability of extended-reach wells is shown in Fig. 13.

From Fig. 13, it can be seen that the rotating speed of the rotary table has little effect on the ultimate extension capability in rotary drilling, but the extension capability varies greatly under different borehole curvatures and different WOB conditions.

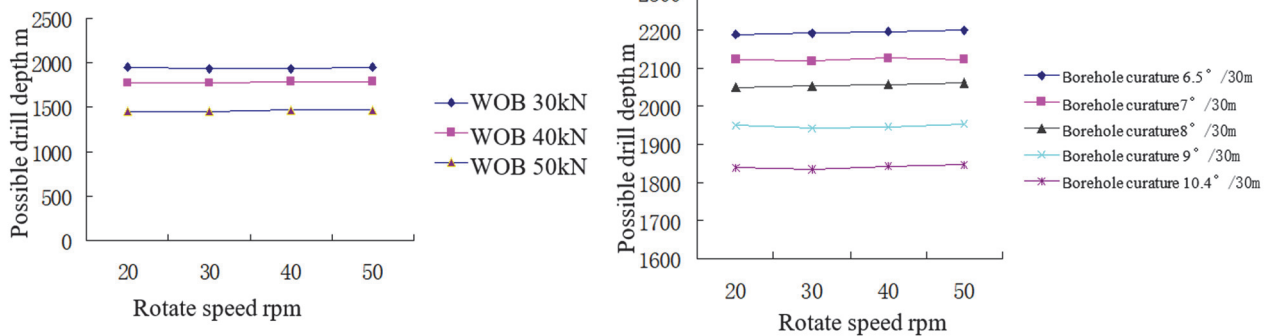


Figure 13 The effect of rotate speed of rotary table on extension capacity of extended-reach well

### 4.2.2 Effect of Borehole Friction Coefficient on the Ultimate Extension Capacity of the Extended-Reach Wells

The coefficient of friction is the most important factor affecting the extension ability of the extended-reach wells. The frictional resistance of the borehole wall to the drill string does not allow the drill string's effective weight to be fully transferred to the drill bit. If the borehole friction coefficient is too large, it will quickly result in the drill bit not receiving sufficient WOB, and the current drill assembly cannot continue to drill. The high coefficient of

friction in this well makes it difficult to drill, resulting in poor extension ability of the extended-reach well and sometimes difficult bare hole drilling. The effect of the borehole friction coefficient on the ultimate extension capability is shown in Fig. 14.

It can be seen from Fig. 14 that the extension ability decreases significantly with the increase of the friction coefficient, and the extent of the decline is large. Compared with the above factors, the borehole friction coefficient has the greatest effect on the stretching capacity.

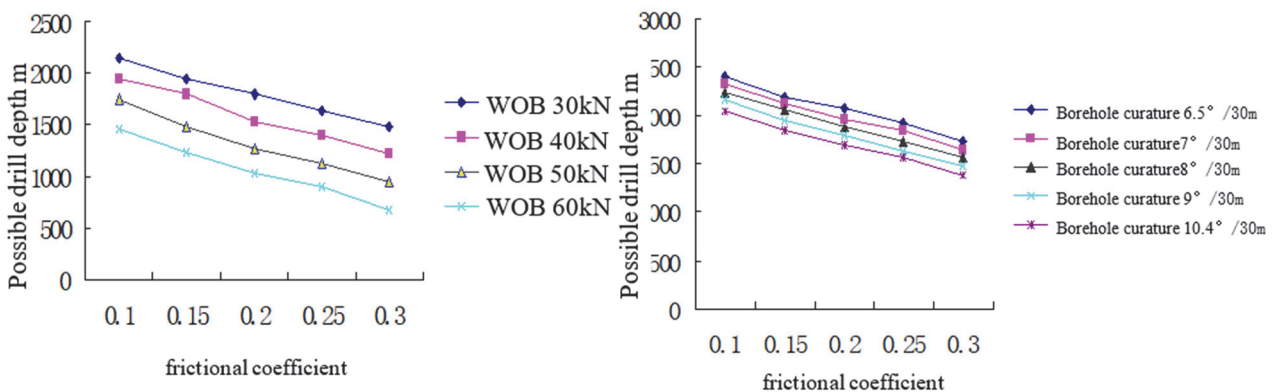


Figure 14 The effect of frictional coefficient on extension capacity of extended reach well

### 4.2.3 The Effect of Borehole Curvature on Ultimate Extent of the Extended-Reach Wells

The borehole curvature is the average wellbore rate of change in the deflected section in the design of the extended-reach well. The actual wellbore is a curved

spatial curve, in such a downhole environment, the extended-reach well drill string is in random contact with the well wall, and the axis of the drill string itself must also bend with the wellbore. It is due to this contact that the friction between the drill string and the well wall increases, thereby affecting the extension capability of the extended-

reach well. The influence of the borehole curvature on the ultimate extension capacity of the extended-reach wells is shown in Fig. 15. It can be seen from Fig. 15, as the borehole curvature increases, the ability to extend

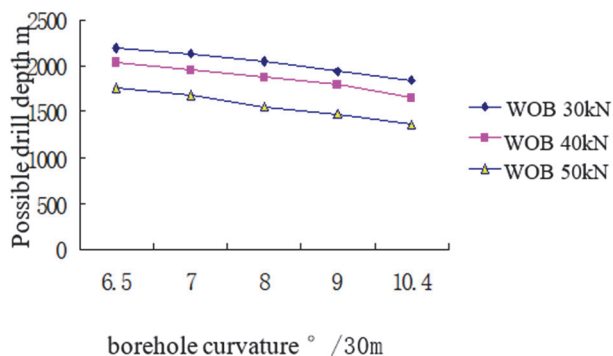
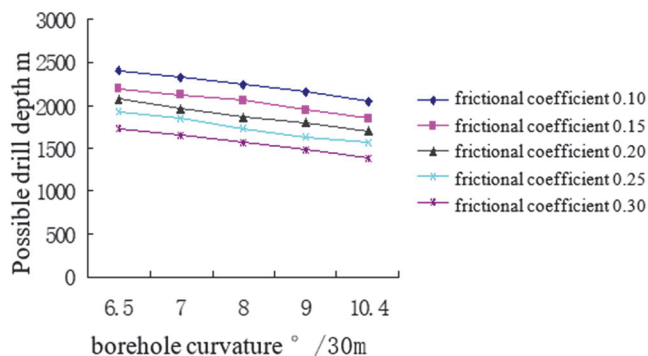


Figure 15 The effect of borehole curvature on extension capacity of extended-reach well



From the above analysis, it is clear that in the design and construction of the extended-reach wells, to ensure the drilling of horizontal sections, the borehole friction coefficient should be reduced as much as possible, and the borehole curvature should be minimized. This requires the use of low-friction drilling fluids and smoother borehole trajectories as far as possible, and the use of rotary drilling whenever possible.

## 5 CONCLUSION

(1) The extended limit prediction criteria for the extended-reach wells are given. This article uses the theory and method of drill string mechanics to study the extended restriction factors of the extended-reach wells and points out that the extended-reach wells are limited by drilling rigs, threshold WOB, frictional resistance, strength, and stiffness.

(2) According to the fact that the drill string mechanics of the extended-reach well is non-linear, the integral drill string finite element method and the gap element method are used to establish the integral drill string static gap element mechanics model for the extended-reach wells. This method simplified the actual downhole conditions less, and it can describe the stress state of the drill string more realistically.

(3) The dynamics finite element method is used to analyze the mechanical model of the drill string of an extended-reach well. This method can quantitatively evaluate and predict the fatigue strength of the drill string of an extended-reach well. The results show that the technique is reliable.

(4) The computer software developed based on the theoretical models can be used to predict and evaluate the distribution law of drill string friction in the extended-reach wells, and to predict the extension limit of the extended-reach wells. It can be seen from the calculation of the actual drilling of the extended-reach wells in the field that the maximum error between the calculation results and the actual measurement is 10.82%, the minimum error is 2.98%, the average error is 6.94%, and the errors are all below 15%. The results show that the calculation results of this method are consistent with the measured results, which

decreases significantly. It can be seen from the relationship curve that the influence of the borehole curvature on the extension ability is smaller than the influence of the friction coefficient.

can meet the requirements of drilling engineering for the extended-reach wells.

## Acknowledgements

Supported by Petro China Innovation Foundation (2017D-5007-0309); Heilongjiang Postdoctoral Scientific Research Developmental Fund (No. LBH-Q20083).

## 6 REFERENCES

- [1] Lubinski, A. (1950). *A study of the buckling of rotary drilling strings*. *Drilling and Production Practice*. American Petroleum Institute, 178-214.
- [2] Arthur, L. & Woods, H. B. (1953). *Factors affecting the angle of inclination and dog-legging in rotary bore holes*. *Drilling and Production Practice*. American Petroleum Institute, 222-242.
- [3] Arthur, L. & Woods, H. B. (1955). *Use of stabilizers in controlling hole deviation*. *Drilling and Production Practice*. American Petroleum Institute, 165-182.
- [4] Arthur, L. (1961). Maximum permissible dog-legs in rotary boreholes. *Journal of Petroleum Technology*, 13(2), 175-194. <https://doi.org/10.2118/1543-G-PA>
- [5] Woods, H. B. & Arthur, L. (1954). *Practical chart for solving problems on hole deviation*. *Drilling and Production Practice*. American Petroleum Institute, 84.
- [6] Finnie, I. & Bailey, J. (1960). An experimental study of drill-string vibration. *Journal of Engineering for Industry*, 82(2), 129-135. <https://doi.org/10.1115/1.3663020>
- [7] Bailey, J. & Finnie, I. (1960). An analytical study of drill-string vibration. *Journal of Engineering for Industry*, 82(2), 122-127. <https://doi.org/10.1115/1.3663019>
- [8] Dareing, D. W. & Billy, J. L. (1968). Longitudinal and angular drill-string vibrations with damping. *Journal of Engineering for Industry*, 90(4), 671-679. <https://doi.org/10.1115/1.3604707>
- [9] Walker, B. H. (1973). Some technical and economic aspects of stabilizer placement. *Journal of Petroleum Technology*, 25(6), 663-672. <https://doi.org/10.2118/4263-PA>
- [10] Bai, J. Z. & Su, Y. N. (1994). Theory and practice of well inclination control. *Beijing, Petroleum Industry Press, 1994*.
- [11] Millheim, K. K., Steven, J., & Ritter, C. J. (1978). Bottom-hole assembly analysis using the finite-element method. *Journal of Petroleum Technology*, 30(2), 265-274. <https://doi.org/10.2118/6057-PA>

- [12] Millheim, K. K. & Keith, K. (1977). The effect of hole curvature on the trajectory of a borehole. *SPE Annual Fall Technical Conference and Exhibition*.  
https://doi.org/10.2118/6779-MS
- [13] Millheim, K. K. (1978). Eight part series on directional drilling. *Oil and Gas Journal*.
- [14] Millheim, K. K. & Apostal, M. C. (1981). The effect of bottomhole assembly dynamics on the trajectory of a bit. *Journal of Petroleum Technology*, 33, 2323-2338.  
https://doi.org/10.2118/9222-PA
- [15] Millheim, K. K. & Apostal, M. C. (1981). How BHA dynamics affect bit trajectory. *World Oil*, 92(6), 183-205.
- [16] Millheim, K. K. (1982). Computer simulation of the directional drilling process. *International Petroleum Exhibition and Technical Symposium*.  
https://doi.org/10.2118/9990-MS
- [17] Dunayevsky, V. A., Judzis, A., & Mills, W. H. (1984). Onset of drill string precession in a directional borehole. *SPE Annual Technical Conference and Exhibition*.  
https://doi.org/10.2118/13027-MS
- [18] Dunayevsky, V. A., Abbassian, F., & Judzis, A. (1993). Dynamic stability of drill strings under fluctuating weight on bit. *SPE drilling & completion*, 8(2), 84-92.  
https://doi.org/10.2118/14329-PA
- [19] Jian, S. H. (1990). Finite element analysis of the lower and middle hole drill assembly of curved wellbore. *Acta Petrolei Sinica*, 4, 95-105.
- [20] Ooms, G. & Kampman-Reinhartz, B. E. (2000). Influence of drill pipe rotation and eccentricity on pressure drop over borehole with newtonian liquid during drilling. *SPE Drilling & Completion*, 15(4), 249-253.  
https://doi.org/10.2118/67618-PA
- [21] Heisig, G. & Neubert, M. (2000). Lateral drill string vibrations in extended-reach wells. *IADC/SPE drilling conference*. https://doi.org/10.2118/59235-MS
- [22] Liu, Q. Y. & Huang, B. S. (2001). Establishment and solution of transverse vibration model of roller bits. *Drilling Engineering*, 21(4), 55-56.  
https://doi.org/10.3321/j.issn:1000-0976.2001.04.015
- [23] Guan, Z. C., Yan, Y. X., & Wang, Y. F. (2003). Experiment study on dynamic state of down drilling column of bottom well. *Acta Petrolei Sinica*, 24(6), 102-106.  
https://doi.org/10.3321/j.issn:0253-2697.2003.06.022
- [24] Han, C. J., Yan, T., & Bi, X. L. (2005). Analysis and application of drill string vibration in deep wells. *Natural Gas Industry*, 25(9), 76-79.  
https://doi.org/10.3321/j.issn:1000-0976.2005.09.025
- [25] Han, C. J., Yan, T. (2005). Study on the lateral vibration law of drill string during horizontal drilling of horizontal well. *Petroleum Machinery*, 33(1), 8-10.  
https://doi.org/10.3969/j.issn.1001-4578.2005.01.003
- [26] Rae, G., Lesso, Jr W. G., & Sapjanskas, M. (2005). Understanding torque and drag, best practices and lessons learnt from the captain field's extended reach wells. *Amsterdam, SPE/IADC Drilling Conference*.  
https://doi.org/10.2118/91854-MS
- [27] Janwadkar, S. S., Fortenberry, D. G., & Roberts, G. K. (2006). BHA and drillstring modeling maximizes drilling performance in lateral wells of barnett shale gas field of N. Texas. *SPE Gas Technology Symposium*.  
https://doi.org/10.2118/100589-MS
- [28] Bakke, O. (2012). A study in limiting factors for extended reach drilling of highly deviated wells in deep waters. *MS thesis*. Institutt for petroleumsteknologi og anvendt geofysikk.
- [29] Abahusayn, M., Foster, B., Brink, J., & Kuck, M. (2012). Nikaitchuq extended-reach drilling, designing for success on the north slope of alaska. *SPE Drilling & Completion*, 27(4), 501-515. https://doi.org/10.2118/149778-PA
- [30] Vestavik, O., Egorenkov, M., & Schmalhorst, B. (2013). Extended reach drilling-new solution with a unique potential. *SPE/IADC Drilling Conference*.  
https://doi.org/10.2118/163463-MS
- [31] Gradishar, J., Ugueto, G., & Van Oort, E. (2014). Setting free the bear, the challenges and lessons of the Ursa A-10 deep water extended-reach well. *SPE Drilling & Completion*, 29(2), 182-193. https://doi.org/10.2118/163525-PA
- [32] Xin, L. (2018). *Basic research on open hole extension limit prediction and control technology of extended reach horizontal wells*. Doctoral Dissertation, China University of Petroleum (Beijing).
- [33] Wenjun, H., Xiaolei, S., & Deli, G. (2020). The subsection optimization design method of pipe string based on drilling extension limit. *Petroleum Machinery*, (04), 1-8.  
https://doi.org/10.16082/j.cnki.issn.1001-4578.2020.04.001

**Contact information:****Weikai LIU**

Department of Petroleum Engineering, Northeast Petroleum University, Daqing high-tech development zone university street No.99, Daqing, Heilongjiang, China  
E-mail: 67809754@qq.com

**Zhiming TIAN**

Department of Petroleum Engineering, Northeast Petroleum University, Daqing high-tech development zone university street No.99, Daqing, Heilongjiang, China  
E-mail: 630458410@qq.com

**Yueqing XU**

Daqing Drilling Engineering and Technology Research Institute, South Babaishang Street No. 37, Daqing, Heilongjiang, China  
E-mail: xuyueqing@cnpc.com.cn

**Min ZHAO**

No. 1 Mud Logging Company of CNPC Daqing Drilling & Exploration Engineering Corporation, Ranghulu District South 3rd Road No. 71, Daqing, Heilongjiang, China  
E-mail: zhaomin007@cnpc.com.cn

**Runqi LI**

Daqing Drilling Engineering and Technology Research Institute, South Babaishang Street No. 37, Daqing, Heilongjiang, China  
E-mail: xuyueqing@cnpc.com.cn

**Haibo PANG**

Daqing Drilling Engineering and Technology Research Institute, South Babaishang Street No. 37, Daqing, Heilongjiang, China  
E-mail: xuyueqing@cnpc.com.cn

**Hongyan ZHAO**

Daqing Drilling Engineering and Technology Research Institute, South Babaishang Street No. 37, Daqing, Heilongjiang, China  
E-mail: xuyueqing@cnpc.com.cn

**Ziming FENG**

(Corresponding Author)  
College of Mechanical and Electrical Engineering, Wenzhou University, Chashan Higher Education Park, Wenzhou City, Zhejiang Province, China  
E-mail: xueyuanfzm@163.com